Journal of Urban and Environmental Engineering
E-ISSN: 1982-3932
celso@ct.ufpb.br
Universidade Federal da Paraíba
Brasil

Deb, Bachu; Gupta, Rajat; Misra, R.D.
PERFORMANCE ANALYSIS OF A HELICAL SAVONIUS ROTOR WITHOUT SHAFT AT 45° TWIST ANGLE USING CFD
Journal of Urban and Environmental Engineering, vol. 7, núm. 1, -, 2013, pp. 126-133
Universidade Federal da Paraíba
Paraíba, Brasil

JUEE

Journal of Urban and Environmental Engineering, v.7, n.1, p.126-133

ISSN 1982-3932
doi: 10.4090/juee.2013.v7n1.126133

Journal of Urban and Environmental Engineering

www.journal-uee.org

PERFORMANCE ANALYSIS OF A HELICAL SAVONIUS ROTOR WITHOUT SHAFT AT 45° TWIST ANGLE USING CFD

Bachu Deb[1*], Rajat Gupta[2] and R.D. Misra[3]

[1] *Ph.D Scholar, Department of Mechanical Engineering, NIT Silchar Silchar - 788010, Assam, India*
[2] *Professor & Director, National Institute Technology Srinagar*
[3] *Professor & Head, Department of Mechanical Engineering, NIT Silchar*

Received 28 December 2012; received in revised form 30 January 2013; accepted 09 February 2013

Abstract: Helical Savonius rotor exhibits better performance characteristics at all the rotor angles compared to conventional Savonius rotor. However studies related to the performance measurement and flow physics of such rotor are very scarce. Keeping this in view, in this paper, a three dimensional Computational Fluid Dynamics analysis using commercial Fluent 6.2 software was done to predict the performance of a two-bucket helical Savonius rotor without shaft and with end plates in a complete cycle of rotation. A two-bucket helical Savonius rotor having height of 60 cm and diameter of 17 cm with 45° bucket twist angle was designed using Gambit. The buckets were connected at the top and bottom circular end plates, which are 1.1 times the rotor diameter. The k-ε turbulence model with second order upwind discretization scheme was adopted with standard wall condition. Power coefficients (Cp) and torque coefficients (Ct) at different tip speed ratios were evaluated at different rotor angles. From the investigation, it was observed that power coefficient increased with increase of tip speed ratio up to an optimum limit, but then decreased even further tip speed ratio was increased. Further investigation was done on the variations of Cp & Ct in a complete cycle of rotation from 0° to 360° in a step of 45° rotor corresponding to the optimum tip speed ratio. The value of Cp at all the rotor angles is positive. Moreover, velocity magnitude contours were analyzed for each rotor angle and it could be concluded that high aerodynamic torque and power can be expected when the rotor is positioned at 45º & 90º with respect to incoming flow.

Keywords: Two-bucket helical Savonius rotor; tip speed ratio; power coefficient; torque coefficient.

* Correspondence to: Bachu Deb. E-mail: bachudeb@gmail.com

INTRODUCTION

The Savonius vertical axis wind rotor was first developed by S. J. Savonius in 1929 (Savonius, 1931). The design was based on the principle of Flettner's rotor. He used a rotor which was formed by cutting a Flettner cylinder from top to bottom and then moving the two semi-cylinder surfaces sideways along the cutting plane so that the cross-section resembled the letter 'S'. To determine the best geometry, Savonius tested 30 different models in the wind tunnel as well as in the open air. The best of his rotor model had 31% efficiency and the maximum efficiency of the prototype in the natural wind was 37%. Bach (1031) made some investigations of the S-rotor and related machines. The highest measured efficiency was 24%.

McPherson (1972) reported a highest efficiency of 33% and the maximum power coefficient obtained by Newman (1974) was only 20%. Modi et al. (1984) reported a power coefficient of 0.22.There had been some works done as to incorporate some modifications in the design of blades so that Savonius rotor may be quite useful for small-scale power requirements. In the last few decades many researchers had worked on the different designs of Savonius rotor and obtained its efficiency in the range of 15%–38%. In the Continuation Grinspan et al. (2001) in this direction led to the development of a new blade shape with a twist for the Savonius rotor. They reported a maximum power coefficient of 0.5. Further Saha et al. (1994) performed experiments on twist bladed Savonius rotor made of bamboo in a low-speed wind tunnel. They showed that their model was independent of wind direction and though the model produced slightly lower rotational speed but easy fabrication of such models made their design suitable for small-scale requirements. Further such design can worth hundred times better than those using deflecting plates & shielding to increase efficiency, which would make the design structurally complex. Again Saha & Rajkumar (2008) performed work on twist bladed metallic S-rotor and compared the performance with conventional semicircular blades having no twist. They obtain C_p of 0.14, which was higher than that of the later with C_p of 0.11. The rotor also produced starting torque and larger rotational speeds. The analysis is done by Hussain et al. (2008) on the enhancement of efficiency by modifying the blade configuration from straight semi circular to a twisted semi circular one. The twist in this turbine is assumed to be given as the bottom cross-sectional surface of the blades is fixed and the top cross-sectional surface is given the desired twist with respect to the bottom fixed surface. Wind flow analysis is done over each configuration of the rotor with the blade twist angles ranging from 5^o to 60^o in steps of 5^o. The optimum angle of twist at which the efficiency and the output power is maximum is evaluated.

Biswas & Gupta (2007) conducted model tests on three-bucket S-rotor, taking tunnel blockage into consideration, and reported maximum power coefficient of 38%. Further Bhaumik & Gupta (2010) studied experimentally the performance of helical Savonius rotor at 45º twist angle in a centrifugal blower. They consider the provision of different overlap ratio from 0.106 to 0.186.It is concluded from their result that maximum C_p is obtained as 0.421 at an overlap ratio of 0.147. Gupta & Deb (2011) studied the CFD analysis of a two bucket helical Savonius rotor with shaft at 45º twist angle. From their study they concluded that the highest values of dynamic pressure and velocity magnitude were obtained at the chord ends with 45^0 bucket twist and 90^0 rotor angle, which would ensure improved performance of the rotor as a whole by increasing the aerodynamic torque production of the rotor. Kamoji et al. (2008) investigates single stages modified Savonius rotorsand concluded that at overlap ratio 0.0 blade arc angle 124º and an aspect ratio of 0.7 has a maximum coefficient of power at a Reynolds number of 1 500 000 which is higher than conventional Savonius rotor.

Keeping this in view, a two-bucket helical savonius rotor without shaft having 45° bucket twist angle was designed. Computational fluid dynamics (CFD) analysis using fluent package was done to analyse the power coefficient and torque coefficient of the rotor at 45° blade twist angle at different rotor angles. Further velocity magnitude contours were analyzed to understand the flow physics of the rotor at different rotor angles.

PHYSICAL MODEL

The three-dimensional model of the two-bucket helical Savonius rotor without shaft at 45° twist angle is shown in **Fig. 1**.The bucket are connected at the top and bottom circular end plates, which is 1.1 times the rotor diameter. There is no central shaft in between the top and bottom plates. Both the inner edge and the outer edge undergo a twist of 45°, a quarter pitch turn. The blade retains its semi-circular cross section from the bottom (0°) to the top (45°). The buckets were spaced 180° apart and were fixed to the end plates. The physical models were designed for five rotor angles namely 0°, 45°, 90°, 135° and 180°. The height of the rotor (H) is 60 cm, radius of the bucket (R) is 8.5 cm, and diameter of the shaft (d) is 3.5 cm.

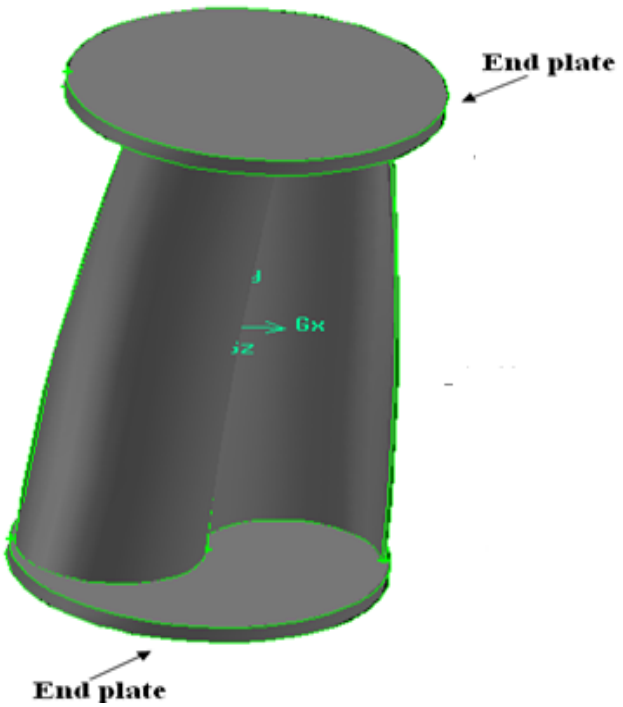

Fig. 1 Helical Savonius rotor without shaft.

COMPUTATIONAL MODEL

Computational Mesh

Three-dimensional tetrahedral mesh around the rotor was developed in the computational modeling of the rotor.

Boundary conditions

At the inlet of the computation zone, uniform velocity distribution is set according to the rated design parameters. The outlets are all set to be pressure outlet where local atmospheric pressure condition is fulfilled. Rotor wall roughness is defined and no slip condition is set at all solid walls.

Table 1: Solution specifications and controls

Boundary condition	Inlet : Velocity Inlet
	Sides : Symmetry
	Bucket : Wall
	Outlet : Pressure Outlet
	Turbulence level: ±1%

Mathematical Formulation

Mathematical model can be defined as the combination of dependent and independent variables and relative parameters in the form of a set of differential equations which defines and governs the physical phenomenon. In the following subsections differential form of the governing equation are provided according to the computational model and their corresponding approximation and idealizations.

Continuity Equation

The conservation of mass equation or continuity equation is given by

$$\frac{\partial \rho}{\partial t} + \nabla.(\rho \vec{V}) = 0 \qquad (1)$$

where ρ is the density, $\vec{V}$ is the velocity vector.

Momentum Equation

Applying the Newton's second law (force = mass × acceleration) the conservation of momentum equation is given by:

$$\frac{\partial}{\partial t}(\rho \vec{V}) + \nabla.(\rho \vec{V} \vec{V}) = -\nabla p + \nabla.\bar{\bar{\tau}} \qquad (2)$$

where ρ is the density, $\vec{V}$ is the velocity vector, p is the static pressure, and $\bar{\bar{\tau}}$ is the stress tensor.

Turbulence Model

In this study Standard k-ε turbulence model has been used with logarithmic surface function in the analysis of turbulent flow (FLUENT, 2005). Momentum equation, x, y and z components of velocity, **turbulent kinetic energy (k)** and dissipation rate of turbulent kinetic energy (ε) have each been solved with the use of the program. All these equations have been made by using the iteration method in such a way as to provide each equation in the central point of the cells, and secondary interpolation method with a high reliability level has been employed. In the present study, the standard k-ε turbulence model with standard wall condition was used.

The standard k– ε equations can be represented as:

$$\frac{\partial}{\partial t}(\rho k) + \frac{\partial}{\partial x_i}(\rho k u_i) = \frac{\partial}{\partial x_j}\left[\left(\mu + \frac{\mu_t}{\sigma_k}\right)\frac{\partial k}{\partial x_j}\right] + G_k - \rho\varepsilon - Y_M \qquad (3)$$

$$\frac{\partial}{\partial t}(\rho\varepsilon)+\frac{\partial}{\partial x_i}(\rho\varepsilon u_i)=\frac{\partial}{\partial x_j}\left[\left(\mu+\frac{\mu_t}{\sigma_\varepsilon}\right)\frac{\partial\varepsilon}{\partial x_j}\right] \quad (4)$$
$$+C_{1\varepsilon}\frac{\varepsilon}{k}(G_k)-C_{2\varepsilon}\rho\frac{\varepsilon^2}{k}$$

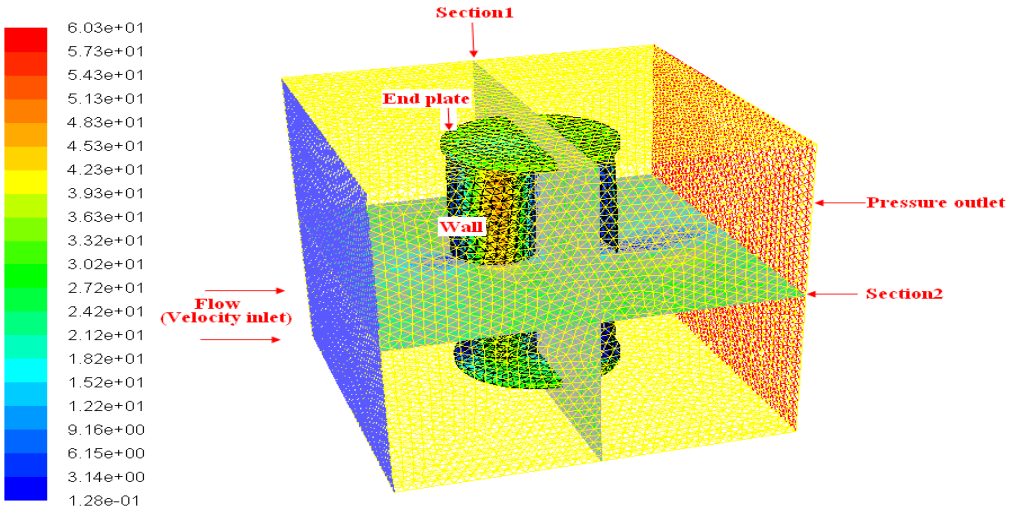

Fig. 2 Computation sections in the 3-D flow field.

In these equations, G_k represents the generation of turbulence kinetic energy due to the mean velocity gradients. Y_M represents the contribution of the fluctuating dilatation in compressible turbulence to the overall dissipation rate. $C_{1\varepsilon}$ and $C_{2\varepsilon}$ are constants. σ_k and σ_ε are the turbulent Prandtl numbers for k and ε , respectively. S_k and S_ε are user-defined source terms.

Computational Zone

A cuboid is applied as the three-dimensional computation body in which the rotor is enclosed. The model is cut through or sectioned by a plane at the centre. Section 1 shows that plane is cut at the centre along the rotor axis i.e. at x = 1, y = 0 & z = 0 similarly section 2 shows that the plane is perpendicular to the rotor axis i.e. x = 0, y = 1 & z = 0. For contour analysis, the data on sections 2 are processed and displayed.

RESULTS AND DISCUSSION

After the convergence of the solution, the power co-efficient (C_p) values are calculated for each value of input air velocity, rotor rotational speed and position of bucket at different rotor angle and tip speed ratio (λ). Following are the equation used to get the power coefficient and torque coefficient.

$$\lambda=\frac{u}{v}=\frac{\pi dN}{60V_{free}} \quad (5)$$

$$T=F_T R=\frac{1}{2}\rho AV^2C_T R=\frac{1}{4}\rho AV^2C_T D \quad (6)$$

$$P_{rotor}=T\omega=\frac{2\pi NT}{60} \quad (7)$$

$$P_{\max}=\frac{1}{2}\rho AV^3 \quad (8)$$

$$C_P=\frac{P_{rotor}}{P_{\max}} \quad (9)$$

Variation of power coefficient at different rotor angle

Figures 3a–3e show below the maximum coefficient of power at different tip speed ratios (λ) whereas **Fig. 3f** shows the variation of coefficient of power in a complete cycle of rotation. Tip speed ratio is defined as the ratio of blade tip speed over undisturbed wind speed. At 0° rotor angle, the maximum power coefficient is 0.0709 at a TSR of 1.636 which is shown in **Fig 3.1**. From **Fig 3.2**, it is seen that for 45° rotor angle, the maximum C_p is 0.462 at a TSR of 1.636. From **Fig 3.3**, it is seen that for 90°rotor angle, the maximum C_p is around 0.2012 at a TSR of 1.636. At 135°rotor angle, the maximum C_p is 0.0080 at a TSR of 0.589 which is shown in **Fig 3.4**. From **Fig 3.5**, it is seen that for 180° rotor angle, the maximum C_p is around 0.073 at a TSR of 1.636. From the figure it was observed that the maximum C_p of 0.4622 occurred at 45° rotor angle at a maximum TSR of 1.636. Further At maximum TSR of

1.636 the variation the power coefficient at different rotor angle in a complete cycle of rotation from 0° to 315° in a step of 45° as shown in **Fig 3.6**. Thus it is seen from **Fig 8** that high power coefficients are obtained at 45º, 90º, 225º and 270º rotor angles, which is responsible for maximum performance of the rotor.

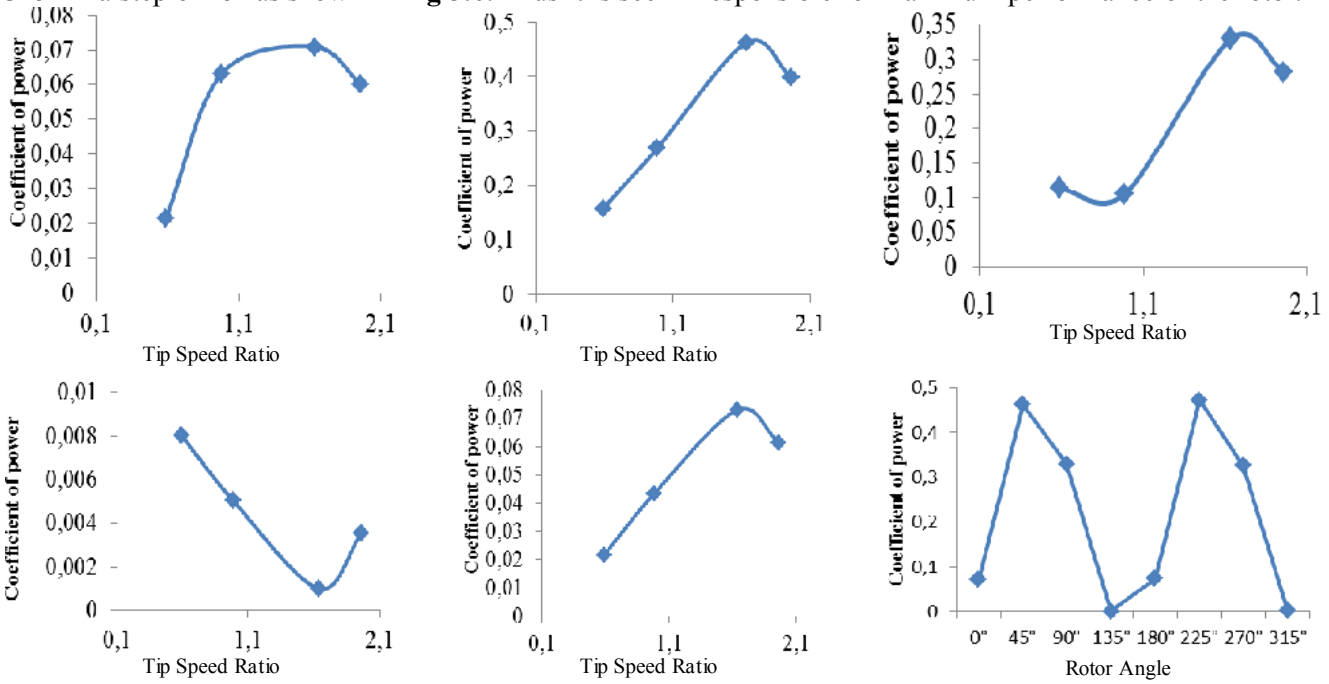

Fig. 3 (a) Variation of C_p at 0° rotor angle with TSR, (b) Variation of C_p at 45° rotor angle with TSR, (c) Variation of C_p at 90° rotor angle with TSR, (d) Variation of C_p at 135° rotor angle with TSR, (e) Variation of C_p at 180° rotor angle with TSR, and (f) Variation of C_p at complete cycle of rotation at maximum TSR=1.636.

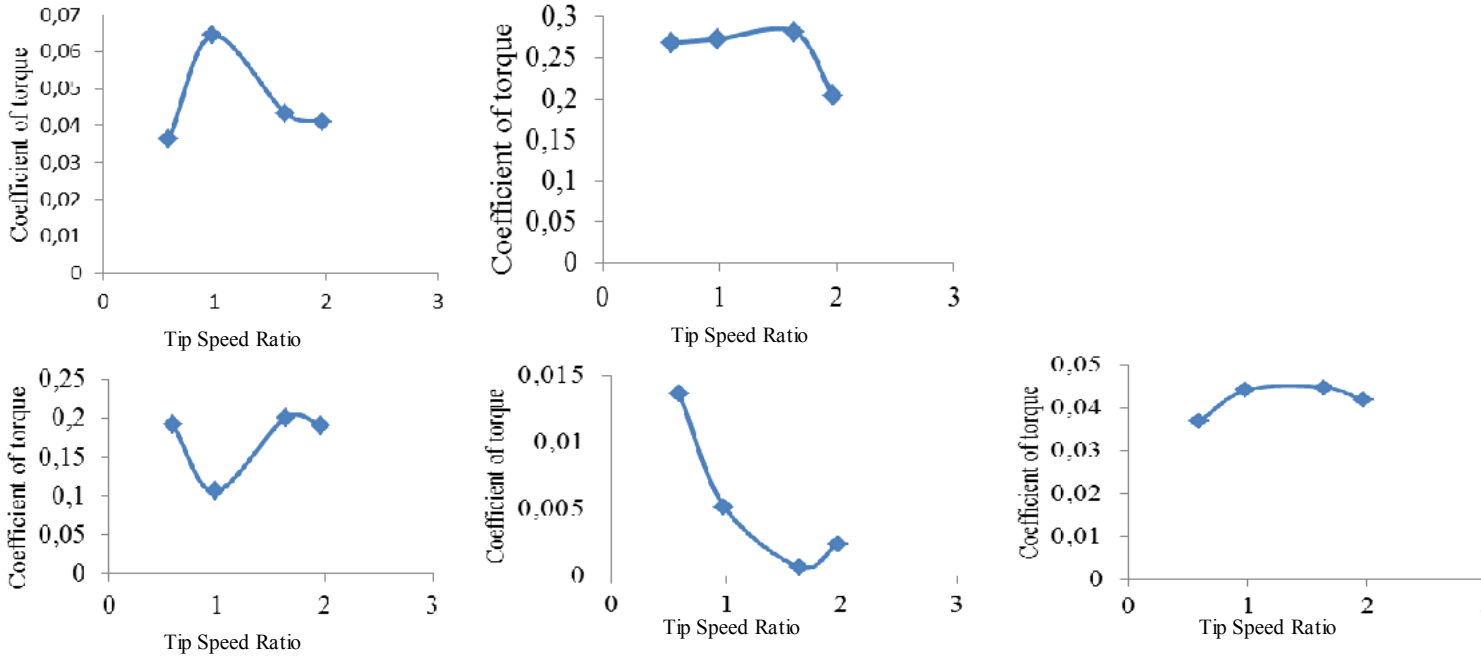

Fig. 4 (a) Variation of C_t at 0° rotor angle with TSR, (b) Variation of C_t at 45° rotor angle with TSR, (c) Variation of C_t at 90° rotor angle with TSR, (d) Variation of C_t at 135° rotor angle with TSR, and (e) Variation of C_t at 180° rotor angle with TSR.

Variation of torque coefficient at different rotor angle

At 0° rotor angle, the maximum torque coefficient (C_t) is 0.0644 at a TSR of 0.981 which is shown in **Fig 4.1**. From **Fig 4.2**, it is seen that for 45° rotor angle, the maximum C_t is 0.282 at a TSR of 1.636. From **Fig 4.3**, it is seen that for 90° rotor angle, the maximum C_t is around 0.2012 at a TSR of 1.636. At 135° rotor angle, the maximum C_t is 0.0136 at a TSR of 0.589 which is shown in **Fig 4.4**. From **Fig 4.5**, it is seen that for 180° rotor angle, the maximum C_t is around 0.0446 at a TSR

of 1.636. From the figure it is observed that the maximum C_t of 0.282 is obtained at 45° rotor angle at an optimum TSR of 1.636.

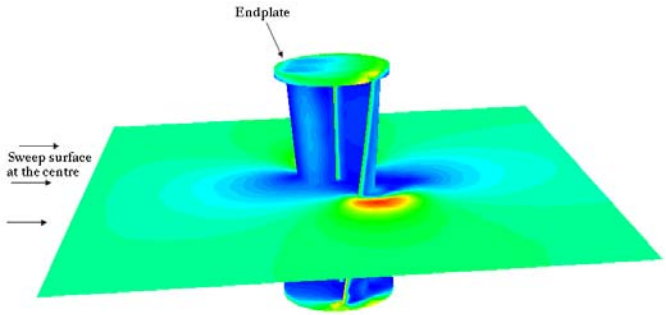

Fig. 5 Sweep surface at centre X=0, Y=1, Z=0

Contour Plot Analysis of helical Savonius rotor without shaft

The contour plots helps to visualize the flow pattern of the fluid in the rotor in an isoplane surface. The isoplane surface is selected at the centre of the rotor at X=0, Y=1, Z=0 as shown in **Fig. 5**.

The contours of velocity magnitude were obtained for five rotor angles namely 0°, 45°, 90°, 135° & 180°. The velocity magnitude contours show that, for all rotor angles, the velocity decreases from the upstream side to the downstream side of the advancing blade. **Fig. 6a−6e** show that velocity magnitudes at the twisted end of the chord increase from 9.64 m/sec for 0° rotor angle to 11.3 m/sec for 45° rotor angle through 11.7 m/sec for 90° rotor angle and then decreases to 11.2 m/sec for 135° rotor angle and finally to 9.6 m/sec for 180° rotor angle. High concentration of velocity distribution occurs near the chord ends which means high aerodynamic torque production by the rotor. Therefore the helical Savonius rotor without shaft at 45° & 90° rotor angle would be responsible for improved performance of the rotor as a whole during its power stroke in the clockwise direction by increasing the aerodynamic torque production of the rotor.

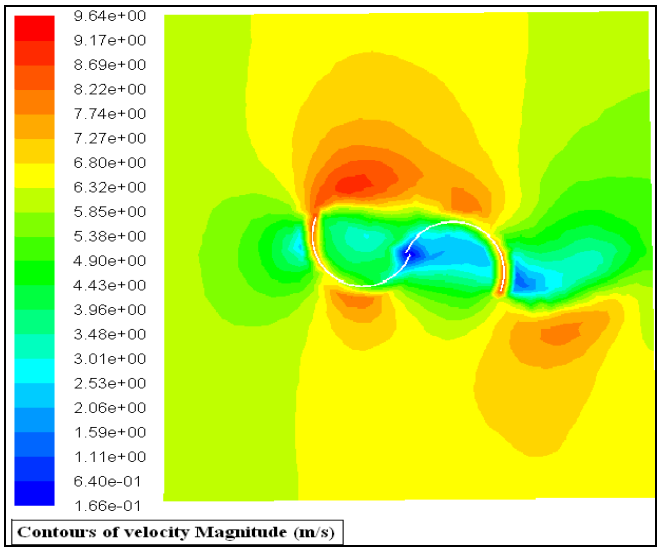

Fig. 6a. Velocity magnitude contour at 0° rotor.

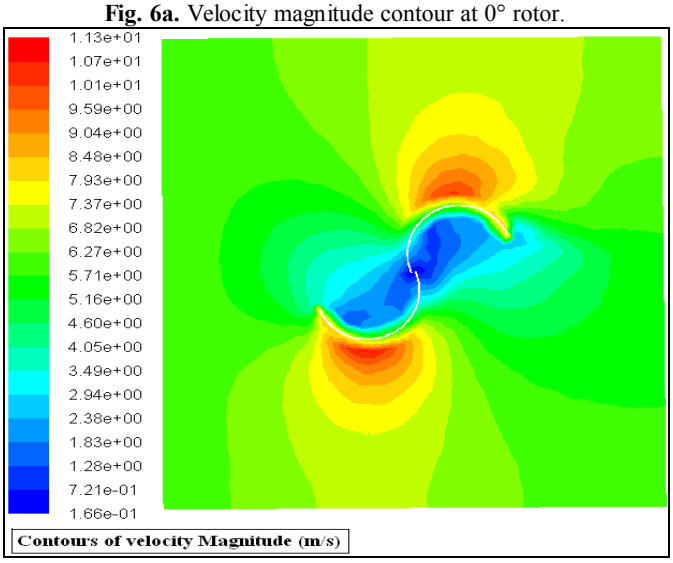

Fig. 6b. Velocity magnitude contour at 45° rotor.

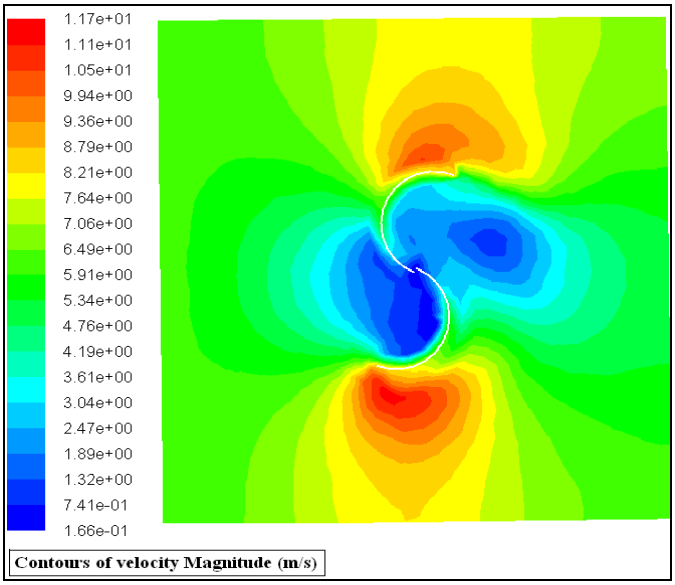

Fig. 6c. Velocity magnitude contour at 90° rotor.

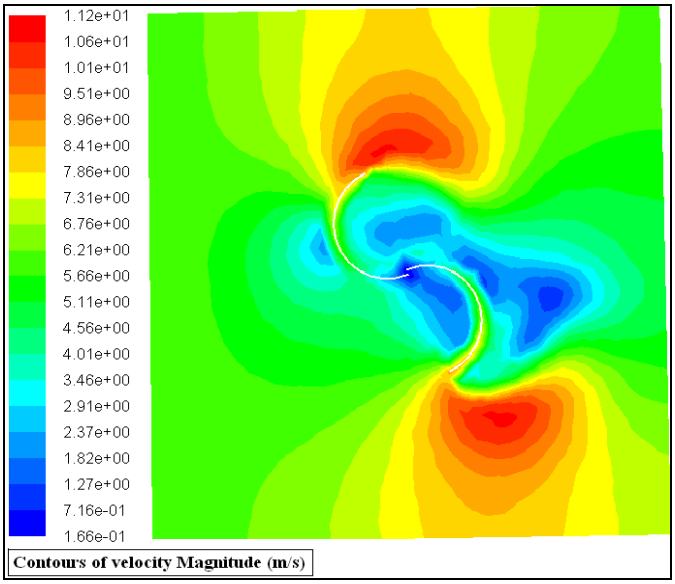

Fig. 6d. Velocity magnitude contour at 135° rotor.

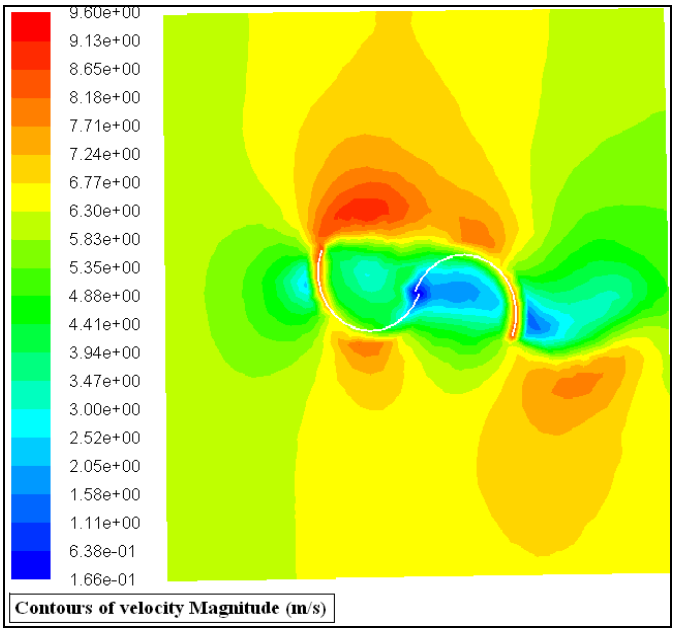

Fig. 6e. Velocity magnitude contour at 180° rotor.

CONCLUSIONS

In this paper, a three dimensional Computational Fluid Dynamics analysis using commercial Fluent 6.2 software was done to predict the performance of a two-bucket helical Savonius rotor without shaft and with end plates in a complete cycle of rotation. From the study, the following conclusions are summarized:

1. The power and torque coefficients obtained at all the rotor angles are positive. Thus, at all rotor angles helical Savonius rotor without shaft produces positive power. Also significant rise in power and torque coefficient occurs at 45º, 90º, 225º and 270º rotor angle. This might be due to favorable pressure gradient across the blades between the end plates.
2. For two bucket helical Savonius rotor without shaft, the maximum power coefficient obtained is 0.462 for 45° rotor angle at a TSR of 1.636.
3. It can be concluded from the contour analysis that the maximum change in concentration of velocity magnitude is from 11.3 m/sec at 45º rotor angle through 11.7 m/sec for 90^0 rotor angle and 11.2 m/sec for 135° rotor angle. Thus, helical Savonius rotor without shaft at 45º & 90° rotor angle would be reponsible for improved performance of the rotor as a whole during its power stroke in the clockwise direction by increasing the aerodynamic torque production of the rotor.

NOMENCLATURE

D	Overall rotor diameter
ρ	Density
d	Bucket diameter of the rotor
r	Bucket radius
h	Height of the Savonius rotor
μ	Viscosity
μ_t	Turbulent viscosity
e	Overlap
A	Swept area
T	Torque
u	Blade rotational speed
P_{rotor}	Power of the rotor
P_{max}	Maximum wind power
ω	Angular velocity
C_p	Power coefficient
λ	Tip speed ratio

REFERENCES

Bach, G. (1931). Investigation concerning S-rotor & related machines. Translated into English by Brace Research Institute, Quebec, Canada

Bhaumik, T, Gupta. R (2010) Performance measurement of a two bladed helical Savonius rotor. Proc. 37th International & 4th National Conference on Fluid Mechanics and Fluid Power FMFP2010 December 16-18, 2010, IIT Madras, Chennai, India.

Biswas, A., Gupta, R., Sharma, K.K. (2007) Experimental investigation of overlap and Blockage effects on Three-Buckets Savonius Rotors. *Journal of Wind Energy* **31**(5), 363-368.

Biswas, A., Gupta, R., Sharma, K.K. (2007). Experimental Investigation of Overlap and Blockage Effects on Three-Bucket Savonius Rotors, *Wind Engineering* **31**(5), 363–368.

FLUENT Inc. Fluent 6.0 documentation: user's guide, 2005.

Grinspan, A.S., Kumar, P.S., Mahanta, P, Saha, U.K., Rao, D.V.R., Bhanu, G.V. (2001). Design, development & testing of Savonius wind turbine rotor with twisted blades. Proc. of 28th National Conference on Fluid Mechanics and Fluid Power, Chandigarh, Dec 13-15, 428-431.

Gupta, R., Deb, B. (2011) CFD analysis of a two-bucket helical Savonius rotor with shaft at 45° twist angle. Sharjah International Symposium of Nuclear and Renewable Energies for 21st Century

(SHJ-NRE11), April 3-5, 2011, College of Sciences, University of Sharjah UAE.

Hussain, M., Nawazish, M.S., Ram, R.P. (2008) CFD analysis of low speed vertical axis wind turbine with twisted blades. *International Journal of Applied Engineering Research* **3**(1), 25-35.

Kamoji, M.A., Kedare, S.B., Prabhu, S.V. (2008) Experimental investigation on single stage, two stage and three stage conventional Savonius rotor. International journal of energy research, **32**:877-895.

Khan, M.H. (1975). Improvement of Savonius Rotor-windmill. M.S. Thesis, University of the Phillipines, Lasbonas.

Macpherson, R.B. (1972). Design, development & testing of low head high efficiency kinetic energy machine- An alternative for the future. University of Massachusetts, Amhest.

Modi, V.J, Roth, N.J, Fernando, M.S. (1984). Optimal configuration studies and prototype design of a wind energy operated irrigation system. *Journal of Wind Engineering and Industrial Aerodynamics*, **16**(1), 85-96.

Newman, B.G. (1974). Measurements on a Savonius rotor with variable air gap. McGill University, Canada.

Saha, U.K., Rajkumar M. (2008) Jaya On the performance analysis of Savonius rotor with twisted blades. *Journal of Wind Engineering and Industrial Aerodynamics*, **96**(8-9), 1359-1375.

Saha, U.K.; Mahanta, P.; Grispan, A.S. (1994) Twisted bamboo bladed rotor for Savonius wind turbines". *Journal of Solar Energy Society of India*, **14**(2): 100-110.

Savonius, S.J. (1931). The S-rotor and its applications, Mech. Engg., **53**(3), 333-338.

Sharma, K.K., Gupta, R., Singh, S.K., Singh, S.R. (2005) Experimental investigation of the characteristics of a Savonius wind turbine. *Wind Engineering*, **29**(1), 77-82.